

Закриті підшипникові вузли для залізничного рухомого складу повинні забезпечувати 800.000 км або 8 років пробігу (а найближчим часом – 1 млн км та 10 років) без будь якого обслуговування. Для досягнення настільки високих експлуатаційних показників необхідно вже під час проектування закритих підшипникових вузлів забезпечити практичну відсутність зносу протягом майже всього вказаного пробігу.

Наведені результати оптимального проектування елементів внутрішньої геометрії закритих підшипників на уточнених математичних моделях на прикладі циліндричного буксового підшипникового вузла «DUPLEX» для рухомого складу простору колії 1520. Основною математичною моделлю було обрано геометричну нелінійну контактну задачу теорії пружності, для вирішення якої авторами використовувався метод скінчених елементів.

Розроблено оригінальну нелінійну скінчено-елементну модель мультиконтактної задачі, яка враховує: контактні деформації «рейка-колесо», деформування осі колісної пари, деформування букси та кілець підшипника при контактній взаємодії зі всіма роликками. Модель дозволяє уточнити розподіл навантажень в окружному напрямку та, відповідно, – максимальне навантаження на ролик. Ця ж модель може бути використана в том числі для аналізу зносу гребня колеса та впливу різноазорності на знос підшипника.

Розроблено математичну модель та цільову функцію для оптимізації профіля ролика («бомбіни», твірної бокової поверхні обертання) з урахуванням накопичення пошкоджень від «нерегулярного» навантаження точок поверхні ролика від контактів як з зовнішнім, так і внутрішнім кільцем.

Проведено оптимізацію форми контактуючих в осьовому напрямку торця ролика та робочого борта кільця, в результаті якої встановлено, що оптимальними є «антропологічні форми» опуклого торця ролика та увігнутого борта кільця. Для технологічного спрощення конструкції замість увігнутого борта кільця прийнято варіант з конічною поверхнею борту з оптимальним значенням «розвалу».

Ключові слова: закритий підшипниковий вузол, бомбіна, ролик, мультиконтактна задача, метод скінчених елементів, математична модель

UDC 539.3, 621.77

DOI: 10.15587/1729-4061.2020.204013

THE REFINED STRENGTH CALCULATION AND OPTIMIZATION OF THE INNER GEOMETRY OF CYLINDRICAL BEARING UNITS

A. Girshfeld

President

JSC «U.P.E.C.»

Marshal Batitskiy str., 4, Kharkiv, Ukraine, 61038

E-mail: anatgir@gmail.com

E. Simson

Doctor of Technical Sciences, Professor, Laureate

of the National Award in the Field of Science and

Technology, Honored Scientist of Ukraine

Department of Continuum Mechanics and

Strength of Materials

National Technical University

«Kharkiv Polytechnic Institute»

Kyrpychova str., 2, Kharkiv, Ukraine, 61002

E-mail: prof.simson@gmail.com

Received date 24.03.2020

Accepted date 28.05.2020

Published date 19.06.2020

Copyright © 2020, A. Girshfeld, E. Simson

This is an open access article under the CC BY license

<http://creativecommons.org/licenses/by/4.0>

1. Introduction

Bearings have probably been the most common units of machines and mechanisms throughout the history of technology development up to now. And their design has very rarely undergone significant changes. One of the recent trends in modern engineering is the use of so-called closed bearing units with prolonged interservice and warranty periods. Thus, for example, closed bearing units for railway rolling stock must operate over a warranty period of 800,000 km or 8 years of operating life (and, in the near future, 1 million km and 10 years) without any maintenance; the failure interval should be at least 1.5 million km; in contrast, conventional axlebox bearings must be serviced after 300,000 km, including oil replacement, rollers rearrangement, analysis of rings for defects; their failure interval is only 600,000 km. It is the savings on regular maintenance and regular repairs that underlies the feasibility of using closed bearing units, which, although more expensive in production and procurement, outperform the rest in terms of a life cycle cost.

However, the advantages of the closed structure turn out to be its main problem at the same time. Because there is no replacement of grease in closed assemblies, the products of roller and ring wear remain inside a bearing unit throughout the warranty period. Thus, once wear products appear, they subsequently work as an abrasive, thereby intensifying the wear almost exponentially. Therefore, in order to achieve such high operational indicators, it is necessary, as early as at the design stage, to ensure not only a reduction but almost absence of wear over all the specified operating life. To this end, it is necessary to apply, practically simultaneously, all possible engineering tools to reduce wear while, at the same time, optimizing elements in the design of a bearing unit applying the refined, rather than simplified, mathematical models.

2. Literature review and problem statement

Constructing a closed bearing unit involves resolving three tasks:

- to design an optimized internal geometry of the bearing to minimize wear amount due to contact stresses;
- to develop a grease that ensures the best compromise between maximum anti-wear properties and minimal hydraulic resistance;
- to design a specialized cassette seal that ensures a similar compromise between a high level of tightness in operation and minimum losses.

Monographs [1–3] academically fully described the analytical methods and mathematical models of bearing calculation for cases of static, dynamic, combined stochastic, and temperature loads. However, all those models have significant simplifications and generalizations, which does not make it possible to apply them directly for optimization.

Paper [4] shows that the classic models and analytical methods of calculating the lifespan of bearings, given in [1–3], do not take into consideration many operational aspects: the great variability of loading scenarios, the inaccuracy of installation, the non-rigid supports, as well as the residual stresses, inadequate conditions of lubrication and the concentration of stresses due to the geometry imperfection. It was proposed to use a finite-element method (FE) as a tool for predicting the service life of surfaces and subsurface layers of rings and rollers; a list of additional problems that could be solved by using an FE method for such prediction was given. However, the cited paper did not directly study the bearing by an FE method; the conclusions are advisory in nature and are not confirmed by research.

The direct analysis of a two-row bearing, applied in the axlebox of high-speed rolling stock, was carried out in work [5]. It is noted that failures of most railway bearings are due to contact fatigue damage caused by the contact stresses between the roller and the ring. The work does not give the dependences of contact stresses on the geometry of its rings and rollers. In addition, the authors did not consider the dependence of service life on the value of contact stress leading to fatigue strains. The construction of a toolset for determining these dependences was addressed in works [6, 7], which proposed a simplified step-by-step algorithm for solving the problem of contact analysis by the FE method in the Ansys software package.

FEM was used in paper [8] to localize the most dangerous zones with a minimum lifespan for a two-row roller bearing. The authors gave a dependence of the projected life of the bearing on the value of a static load. They defined the dependence of contact stress and service life on the inaccuracy of the shape of the raceway of the inner ring. However, the optimization method, proposed in the cited paper, appears insufficient as the bearing model was simplified to the model of interaction between a single roller and a symmetrical sector of the ring; it cannot take into consideration the interaction between roller faces with the flanges of the rings. Such a serious simplification of the model is due to the fact that computation in the Ansys software package is extremely time-consuming, which limits its wide application for the calculation of complete models.

To address the issue of reducing modeling time, work [9] compared the calculation results of two-dimensional and three-dimensional models of bearings. It is noted that the two-dimensional and three-dimensional models produce similar results in certain cases. At the same time, the cited work does not provide criteria for the possibility of using a two-dimensional model. Article [10] reports the analysis of a cylindrical roller bearing and suggests simplifying the geom-

etry of the model to speed up the calculation. The authors established the distribution of contact pressures and projected lifespans for rings and rollers. However, the cited article uses a very rough grid, which calls the results into question. The ideas, proposed in papers [8–10], to simplify the model at the cost of reducing the accuracy of calculation look doubtful.

A mathematical model of contact analysis of ball and roller bearings is proposed in work [11]. The authors gave a simplified procedure of solving the contact problem based on linear elastic FE calculation of the Hertz alternative theory. They analyzed the edge effect at the ends of the non-crowned (non-convex cylindrical) roller. To reduce maximum stresses, it is proposed to use the Joston Goar profile. The cited work does not provide a justification for the optimal application of this particular profile, nor does it consider the effect exerted by the end of the roller of this profile on the side flanges of the rings.

In all the above papers, the studies involved a certain theoretical method without comparing the data obtained with the data acquired by any other method.

Works [12, 13] report the comparison of results obtained by different calculation methods. Paper [12] compared the distributions of stresses and deformations of the roller bearing obtained by the classical analytical method, by a finite element method, as well as experimentally. It is shown that the values of radial deformations closest to the experimental data were obtained by a finite element calculation taking into consideration the elastic deformation of rings. The distribution of static load among rollers was identical under all methods, but the distribution of a radial deformation among rollers, determined by a finite element method with elastically-deformable rings, is significantly (up to 60 %) different from the results obtained in line with Harris, Palmgren, as well as by the method of finite elements with the assumption that the rings are rigid. Paper [13] studied the effect of a radial load, the ambient temperature, and a gap, on the deformation of the inner and outer bearing rings, as well as the stress on the raceways and the rigidity of the bearing. The authors compared the values of the bearing radial deformation, obtained experimentally, analytically in line with Harris, and by a finite element method with elastic rings. Similar to work [12], it is noted that the results obtained by a finite element method are much closer to experimental. The authors of [12, 13] conducted a diversified study, but both papers considered only one type of bearing, making numerical results of their studies inapplicable to investigating bearings of other geometries.

Work [14] studied the operation of a roller bearing as part of the K5 freight car trolley by an FE method. The study involved two stages. In the first stage, the authors modeled a dynamic system consisting of an adapter, bearing, axis, wheel, and rail, but the bearing was modeled as a non-deformable solid body. The authors used the established experimental forces in the contact wheel-rail while moving along a test section of the straight line and curve with a radius of 300 m for 8 seconds. In the second stage, they modeled the bearing operation; the data on the stressed-strained state in the cross-section of a wheelset were used as the boundary conditions. It is noted that the most stressed points are located at the ends of the rollers (an edge effect). After obtaining the maximum stress intensity, the expected lifespan of the bearing elements was determined. The cited work is a validation study, making it possible to determine with high accuracy the service life of a certain bearing under certain operating conditions, but it does not solve the optimization problem.

A simplified method of determining the dependence of the contact stress and radial rigidity of a roller bearing on the convex shape of the roller surface was constructed in article [15]. A mathematical model is given, which makes it possible to solve the roller-raceway contact problem analytically by the method of finite segments. The authors established the dependences of radial rigidity on the bearing load for various forms of “crown”. It is argued that the most rigid are bearings with a logarithmic shape of the roller surface. The article compares the results obtained by various theoretical methods; no experimental testing of the results was carried out. The simulation was carried out for a bearing section with a single roller, without taking into consideration the impact of the axial forces.

Work [16] reports a mathematical quasi-static model of the two-row roller bearing. The authors compared bearing rigidity under the radial and instantaneous loads at radial and angular deformation. The effect of the radial gap and radial load on the bearing service life was considered. The authors considered the effect of the angular inaccuracy of installation and the radial load on the service life of the bearing. However, the cited work did not determine the effect exerted on the bearing lifespan directly by the geometry of rings and rollers. The authors used the simplest rectangular geometry of the raceway cross-section, as well as a cylindrical roller, whose non-optimal shape has been proven by many authors previously.

Papers [17, 18] studied the contact stressed state of an individual bearing in contact with the raceways of the inner and outer rings and the optimization of the roller generatrix; the cited papers preceded our research.

Article [19] modeled bearings with rollers of different shapes; a distribution of contact stresses was obtained for each bearing type. The greatest maximum contact stress was obtained at the ends of a conventional roller, in the place where the inner ring has the lowest thickness. Experimentally, a 1.67-time increase in the lifespan of the bearing was established, when using a roller with the optimal surface shape. The cited article used a simplified static model with a single roller, which does not take into consideration the axial forces. As such, the optimization in that article comes down to a choice of several variants.

Many of the above works compared the contact stresses between a roller and a raceway, obtained by an FE method and analytically (using Hertz theory) with very different conclusions about the meaning of the discrepancies, which makes it impossible to interpret their results unequivocally. Most studies focus on the isolated contact between a single roller and an external or/and external ring. Some papers consider a problem with a full set of rollers, replaced, however, by the estimated rigidity, which, of course, is not equivalent to a multi-contact study. Practically, none of these works consider a simultaneous multi-contact deformation with the elastically deformable rings and axlebox in contact with the outer ring, as well as the deformed axle, wheel in contact with the rail. Instead of full optimization, several variants are typically compared. Except for work [19], the problem of optimizing the axial contact of the roller’s face with the flanges of the inner or/and outer rings is not considered. Work [19] considers the contact with only one ring and only for an almost insignificant case “convex flange–flat face of the roller”.

Thus, it can be concluded that the main interest is to solve a problem that takes into consideration the simultaneous multi-contact deformation with the elastically deformed rings and axlebox in contact with the outer ring, as well as the deformed axle, wheel in contact with the rail.

3. The aim and objectives of the study

The aim of this study is to optimally design all elements in the internal geometry of closed bearings, which would make it possible to ensure a maximum reduction of wear and thus prolong the maximum service life.

To accomplish the aim, the following tasks have been set:

- to construct the refined mathematical models of the contact stressed-strained state (SSS) of rollers and rings, taking into consideration the features of loaders of different structures;
- to optimize the “crown” (of side surface) of the roller in order to maximally minimize the contact stresses;
- to optimize the rounding of the roller face in order to maximally reduce wear in the axial contact with the working flange of the ring.

4. Construction of the refined mathematical models of the contact stressed-strained state (SSS) of rollers and rings taking into consideration the features of loaders of different structures

The principal mathematical model is a geometrically non-linear contact problem from the theory of elasticity, which was solved by using a finite element method (FEM). The physical equations of the Hook’s law are adopted in the matrix form $\sigma=K\varepsilon$, where σ is the vector-column of stresses; K is the matrix of elastic constants; ε is the vector-column of deformations, and the Cauchy geometric equations are taken in the form $\varepsilon=L u$, where u is the vector-column of displacements; L is the differential matrix operator, which, for a three-dimensional finite element, takes the following form:

$$L = \begin{bmatrix} \partial/\partial x & 0 & 0 \\ 0 & \partial/\partial y & 0 \\ 0 & 0 & \partial/\partial z \\ \partial/\partial y & \partial/\partial x & 0 \\ 0 & \partial/\partial z & \partial/\partial y \\ \partial/\partial z & 0 & \partial/\partial x \end{bmatrix}. \tag{1}$$

In this case, the displacements within the u element are expressed through the nodal displacements V^e using the functions of shape N of the finite element $u=N V^e$. The algorithm for implementing a contact with slippage $\mu |F_n|=|F_s|$ was accepted, where F_n and F_s are, respectively, the normal and tangential forces in a gap; μ is the friction factor. $F_n=k_n(u_{n,J}-u_{n,I}-\Delta_n)$, where k_n is the normal rigidity, introduced as a real constant; $u_{n,I}$ is the displacement of node I in the direction of normal; Δ is the gap in the normal direction. $F_s=k_S(u_{S,J}-u_{S,I}-\Delta_0)$, where k_S is the “lock stiffness”; $u_{S,I}$ is the displacement of node I in the tangent direction; $u_{S,J}$ is the displacement of node J in the tangent direction, Δ_0 is the gap in the tangent direction. In this case, the rigidity matrix for such a boundary element in the local coordinates of the element takes the following form (2):

$$[K_l] = \begin{bmatrix} 0 & 0 & 0 & 0 \\ 0 & k_n & 0 & -k_n \\ 0 & 0 & 0 & 0 \\ 0 & -k_n & 0 & k_n \end{bmatrix}. \tag{2}$$

The case when the boundary element is locked and does not slide along the contact is described by inequality $\mu|F_n| \geq |F_s|$, and the corresponding rigidity matrix takes the following form (3).

$$[K_i] = \begin{bmatrix} k_s & 0 & -k_s & 0 \\ 0 & k_n & 0 & -k_n \\ -k_s & 0 & k_s & 0 \\ 0 & -k_n & 0 & k_n \end{bmatrix} \quad (3)$$

Fig. 1 shows the scheme of a one-dimensional contact; Fig. 2–4 show the schemes of a two-dimensional contact. A combined penalty method using Lagrange multipliers was used to determine normal force.

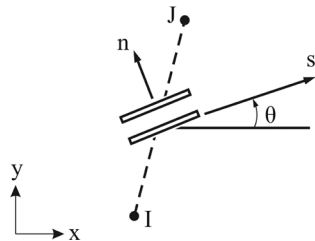


Fig. 1. Scheme of one-dimensional contact

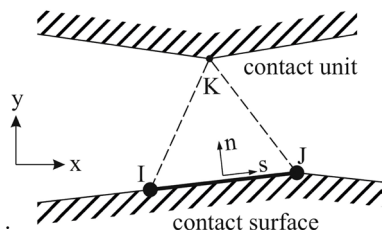


Fig. 2. Scheme of two-dimensional contact

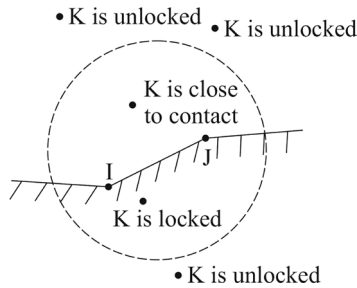


Fig. 3. Scheme of the point entering and exiting a contact

In standard, simplified calculations, the contact problem was considered only for one, the most strained, roller in contact with the inner or/and outer ring. In this case, the distribution of load over a bearing's rollers (in the circumferential direction) is taken in the form of a trigonometric ($\cos\psi$) or parabolic function (Fig. 5). In this case, the maximum load on a roller is taken in the form $Q_{max} = 4.06F_r/z$.

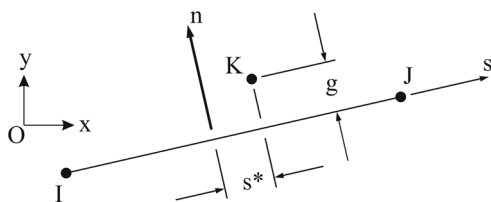


Fig. 4. Scheme of two-dimensional contact

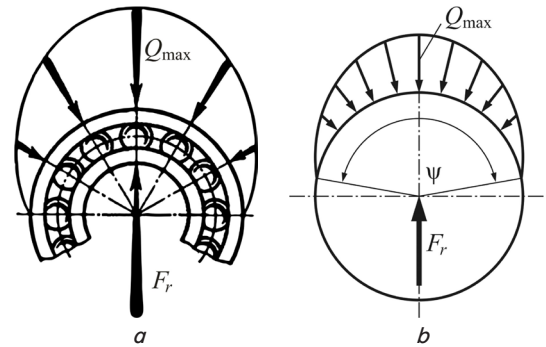


Fig. 5. The distribution of load over rollers: *a* – in the absence of a radial gap; *b* – with a radial gap; Q_{max} is the maximum value of the radial load on a roller; F_r – the total load on a bearing (on a row of rollers); z – the number of rollers

In this case, the average value of the load on a roller $Q_{mid} = 2.49F_r/z$. In the absence of a radial gap, the contact angle ψ is considered to be 180° ; the emergence of a gap naturally reduces the capture angle of the contact, increasing Q_{max} to $5F_r/z$, and Q_{mid} to $2.8F_r/z$.

This study considers a refined approach in the form of the calculation of a multi-contact problem, taking into consideration the simultaneous contact between all rollers and both rings (internal and external). Moreover, the estimation model includes a loader itself (various designs of the axlebox housing or a semi-axlebox/adaptor – for the case of modeling and optimizing a tapered cassette). Only this approach makes it possible, not in a rough approximation but in the refined fashion, to realize both the pattern of load distribution over all rollers in the circumferential direction and the field of contact stresses for the most loaded roller. At the same time, one can see the effect exerted by the structure of a loader on the distribution of loads over rollers and, thus, give preference to a particular design of the axlebox box or semi-axlebox.

Since the total number of degrees of freedom in the model, and, most importantly, the units of non-linear contact elements in the estimated model becomes huge, it is very important to apply all kinds of symmetry and, above all, the symmetry relative to the vertical middle plane of an axlebox. Only the unevenness of load in the axial direction, caused by the bend of the axle of a wheelset under the influence of the car weight, can “interfere” with this symmetry.

To investigate this aspect of modeling, a unique model was formed, including a wagon wheel, which is in contact with the rail, the axle of a wheelset, the assembled bearing, and the axlebox. The load diagram is shown in Fig. 6; the estimated model is shown in Fig. 7. Given that this model is not designed to calculate local contact stresses, in most areas a rather large FE breakdown was used. In addition, the symmetry of loading and the geometry of a wheelset was considered relative to the vertical plane passing in the middle of a wheel axle.

As a result of the calculation, it was found that the inclination angle of the axlebox support section did not exceed 3 minutes, which makes it possible to consider the loading coming from the side frame, almost symmetrical relative to another vertical plane passing through the middle of the axlebox perpendicular to the axle.

Thus, the established symmetry of the bearing unit and loading in two vertical planes made it possible to use a model that consists of the internal and external semi-rings and one-quarter of the axlebox.

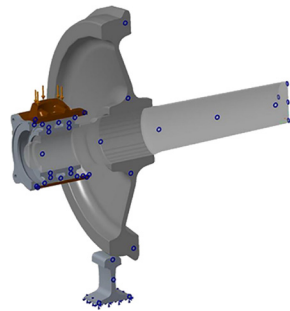


Fig. 6. Load diagram

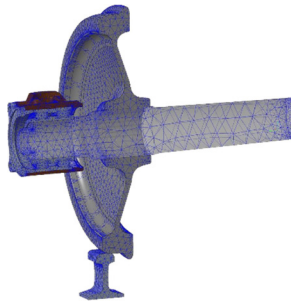


Fig. 7. Estimated model

Initially, the distribution of load and contact stresses over rollers in the closed cylindrical bearing unit CRU Duplex was investigated, placed in the axlebox 100.10.009-0, designed by “Uralvagonzavod” (Russia). The chosen estimated scheme is shown in Fig. 8.

The estimated scheme has the following features:

- the inner surface of the inner ring of the bearing is rigidly fixed according to the arrangement onto a wheel axle;
- a payload of 30.65 kN, equivalent to loading 25 tons per axle, is applied from above at the respective sites;
- the contacts between rings and rollers, as well as between axlebox and the outer ring of the bearing, were considered with and without friction. The “frictionless” type was used in the final calculations due to a slight difference.

The calculations employed an even finite-element grid consisting mainly of hexahedra (Fig. 8, *b*). In most calculations, the size of the finite elements was ~3 mm, the rollers and rings – less than 2 mm. The finite-element estimated model consisted of approximately 220,000 finite elements, including contact ones. To calculate the distribution of efforts over each roller, the inner surface of the outer ring was divided into sectors. It is assumed that the contact area of the roller with the ring is in the middle of the sector. The calculation of each sector determined the average amount of stresses, normal to the surface, which was then multiplied by the surface area of the sector in order to obtain integrated efforts in each sector. The static balance of forces was additionally checked on the vertical axle after designing. To obtain normal stresses, an additional cylindrical coordinate system was introduced, whose polar axis is directed along normal to the surface of the ring. Contact stresses are determined as a result of calculation without the introduction of an additional system of coordinates.

Initially, the calculations were performed without taking into consideration rollers No. 7, 8, or even without three rollers No. 6–8, because the simplified model suggests that the loading does not pass into the lower half of axlebox. Subsequently, refined calculations were carried out taking into

consideration the contact of the rings with all the rollers and a realistically-minimal gap (Fig. 8, *a, b*).

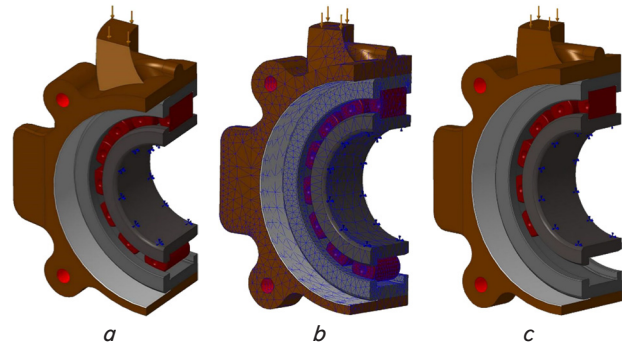


Fig. 8. The estimated model CRU Duplex, placed in the axlebox 100.10.009-0: *a* – taking into consideration a contact with all rollers; *b* – a sample of the finite-element grid; *c* – excluding rollers No. 7, 8

For the case of 14 rollers (Duplex 130×250), the approximate scheme (Fig. 5) produces a maximum load value on the roller on the first, vertically located, roller, of magnitude $Q_{max}=29...36\% F_r$, depending on the size of a gap. The calculation using the refined model shows that the maximum value can be achieved not on a vertically positioned roller but, depending on the size of a gap, on the “second” one, located under the center of the main platform of the axlebox. In this case, the maximum load value is slightly lower than that using the simplified model $Q_{max}=28...34\% F_r$. Below is the distribution of efforts over the most loaded “upper” rollers for the simplified FE model with discarded lower rollers, for a more detailed FE grid (the FE size is up to 1.5 mm), and the refined FE model with a minimum gap, in which all the rollers are in contact.

Table 1

Distribution of efforts over 5 rollers in percentage

Conditional No. of sector/roller	Estimated scheme		
	Without rollers 6–8	Fine grid	All rollers ‘0’ gap
1	34.4 %	31.6 %	21.5 %
2	22.3 %	23.5 %	28.5 %
3	8.5 %	8.8 %	10.2 %
4	1.9 %	1.8 %	0.6 %
5	0.1 %	0.1 %	0.0 %

Fig. 9 shows the same information graphically (“Row 1” – without bottom rollers; “Row 2” – with a more accurate (thick) grid of finite elements; “Row 3” – for the refined model, in which all the rollers are in contact).

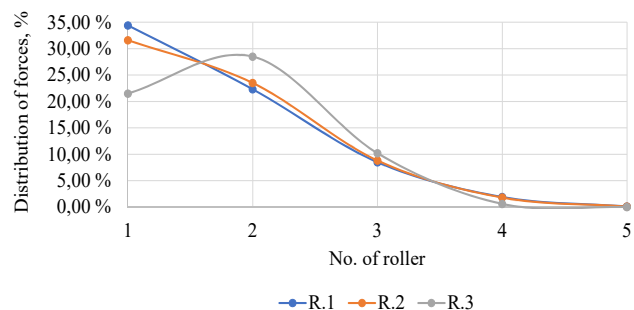


Fig. 9. Distribution of efforts for different estimated FE models

Given the effects detected, further calculations involving an analysis of different forms of loaders were performed for the refined FE model when all the rollers come into contact with the rings. In addition to the main structure of the axlebox 100.10.009-0 designed by “Uralvagonzavod” (“Row 4”), the spatial shapes of the loading site were considered, applied in the semi-axleboxes 50.194.00507, designed by “Uralvagonzavod” (“Row 1”), 1711.10.003, designed by “Specialized Design Bureau of Carriage Engineering named after V. M. Bubnov” (Russia) (“Row 2”), 194.00.053-0, designed by “Uralvagonzavod” (“Row 3”); the results of load calculations for them are shown in Fig. 10 in the form of charts of projection of forces on a vertical axis.

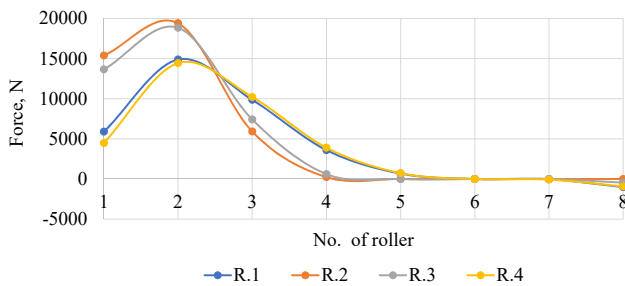


Fig. 10. The distribution of efforts over rollers (in projections on a vertical axis) for different loaders

It can be concluded that in terms of the uniform distribution of loads and, therefore, reducing the maximum efforts and, accordingly, the maximum contact stresses in a bearing unit, the shape of the loading site, applied in the axlebox 100.10.009-0 and semi- axlebox 50.194.00507, is quite rational.

5. Optimization of the side surface of the roller (“crown”) to minimize contact stresses

Previously, the problems on optimizing the generatrix of the roller rotation side surface (so-called “crown”) were considered [17]. However, given the non-linearity of the contact problem, any refinement of the magnitude of a maximum load on the roller leads to a non-linear change in the pattern of contact stresses, and, then, accordingly, the optimal shape of a crown. Thus, as the load distribution model is refined in the circumferential direction, it is necessary to consider refinements to optimize the profile of the roller.

First of all, it is necessary to determine which contact is critical for the accumulation of damage – with an outer or internal ring. As regards the level of maximum contact stresses, it is ~13 % higher in the contact with the inner ring (Fig. 11, a), which is logical from the point of view of internal geometry. However, on the other hand, the number of “inputs” of the roller into the zone of maximum stresses with the outer ring per unit of time (for example, over 1,000 km of mileage) is much higher than into the zone of maximum stresses with an internal ring. The results of the corresponding calculation are shown in Fig. 11, b.

Work [17] concludes that contact with the outer ring should be used as a critical one with a reference to the radical difference in the number of loading per unit of time. However, two important circumstances are not taken into consideration.

First, the accumulation of damage, as well as the Weller curve, prefers a decrease in strains compared to the number of cycles, following an almost linear dependence between the stresses and the logarithmic axis of cycles. Thus, the

four-fold difference in the number of loading is close to compensating for the lower stress value.

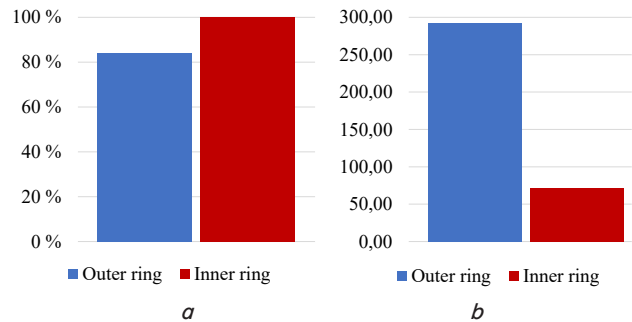


Fig. 11. Comparison: a – the level of maximum contact stresses; b – the frequency of maximum loads

Second, the task of this study is to optimize the profile of the roller, not the ring. A crown (side surface) of the roller in the process of operation rolls sequentially, through a maximum load both with the inner and outer rings, thereby accumulating the damage from both types of peak contact loads. Thus, the optimization should imply not an alternative to a contact with the internal or outer ring, but on the principle of accumulating damage.

As it is known, one of the most used adjusted linear hypothesis of damage accumulation under irregular loading takes the following form:

$$a_p = \int_{\sigma_a} \frac{dn(\sigma_a)}{N(\sigma_a)}, \tag{4}$$

where $dn(\sigma_a)$ refers to the integration for the number of cycles that act with a given stress amplitude σ_a , and $N(\sigma_a)$ is the number of cycles before destruction under the action of variable stresses of amplitude σ_a .

Of course, in the absence of analytical expressions and experimental fatigue curves, integration was replaced without a significant loss for accuracy with a discrete summation by Simpson. Formula (4) actually serves as a criterion for optimizing the profile of the roller (the generatrix).

The distribution of load in the circumferential direction, including the maximum value itself, was used as a result of using the refined multi-contact model described in the previous chapter. In calculating and optimizing the roller profile, another FE model was applied with natural condensation in the immediate contact area, as shown in Fig. 12, 13, using the presence of two instantaneous symmetry planes.

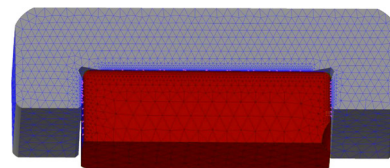


Fig. 12. FE grid in contact with the outer ring (quadrant of symmetry)

Fig. 14, 15 show a pattern of the intensity of contact stresses for a standard “little-crown” roller in contact with the inner (Fig. 14) and outer (Fig. 16) rings. The results show a clear effect of stress concentration. One can see it better in Fig. 15, 17, where the fragments highlighted by a red frame in Fig. 14, 15, respectively, are shown larger below.

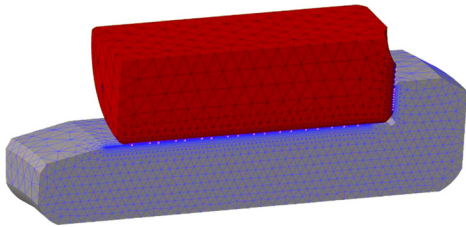


Fig. 13. FE grid in contact with the inner ring (quadrant of symmetry)

The optimization was carried out by the Nelder Mead method by the direct variation of vertical coordinates of the 10 nodal profile points, shown by the spline.

Fig. 18 shows the result of optimizing the profile of a cylindrical roller of the Duplex bearing based on the total criterion (4), which, as the figure shows, is very little different from the previous results of optimization [21]. This is easily explained by the fact that previously [21] found a slight difference in the optimal profile for the criterion of minimizing maximum stresses in the contact between a roller and the internal and outer rings. As a result, the refined approach with criterion (4), which combines the accumulation of damage from loading the roller in contact with the internal and outer rings, has yielded almost the same results.

Fig. 19 shows a pattern of contact stresses for the optimal roller profile, which indicates an extremely equally stressed contact, which is clearly seen in the highlighted fragment (Fig. 20).

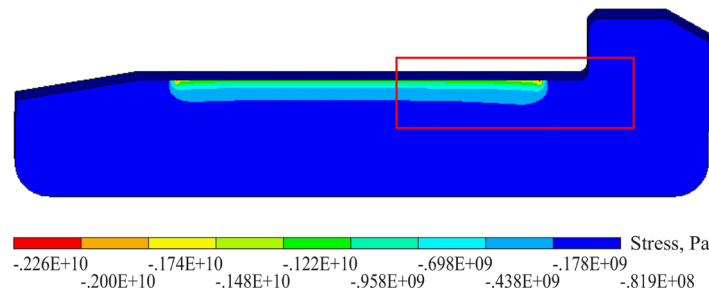


Fig. 14. The intensity of contact stresses for a standard roller in contact with the inner ring

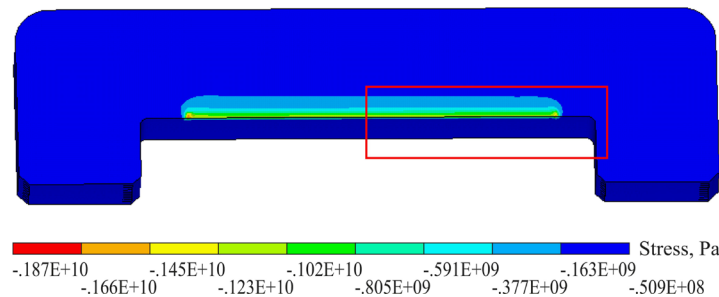


Fig. 15. The intensity of contact stresses for a standard roller in contact with the inner ring (enlarged)

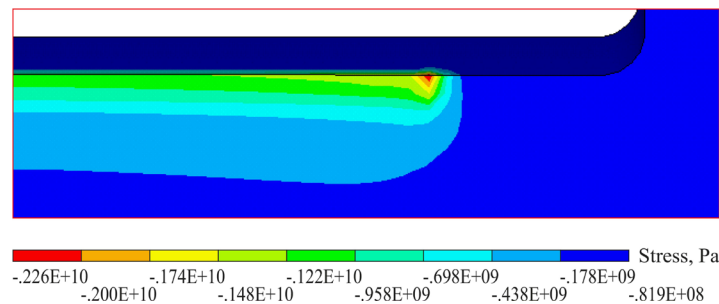


Fig. 16. The intensity of contact stresses for a standard roller in contact with the outer ring

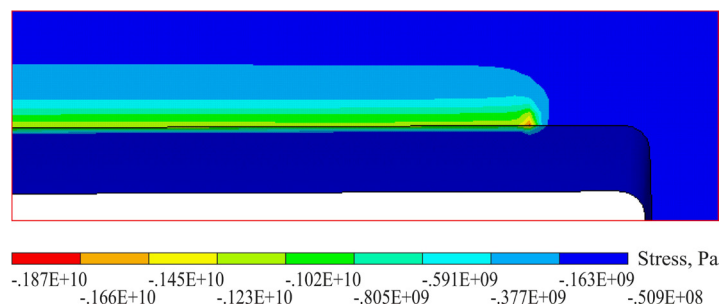


Fig. 17. The intensity of contact stresses for a standard roller in contact with the outer ring (enlarged)

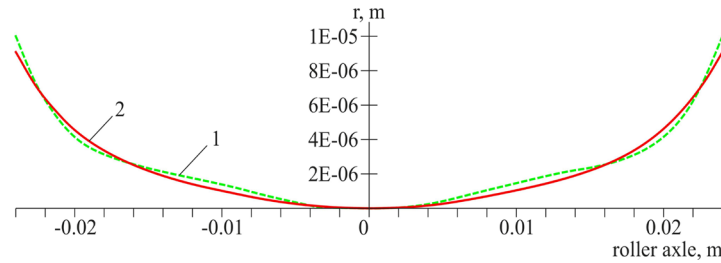


Fig. 18. The result of optimizing the profile of a cylindrical roller of the Duplex bearing

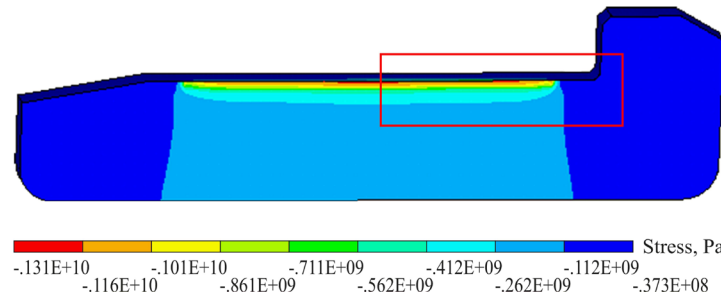


Fig. 19. The intensity of contact stresses for the optimal roller profile

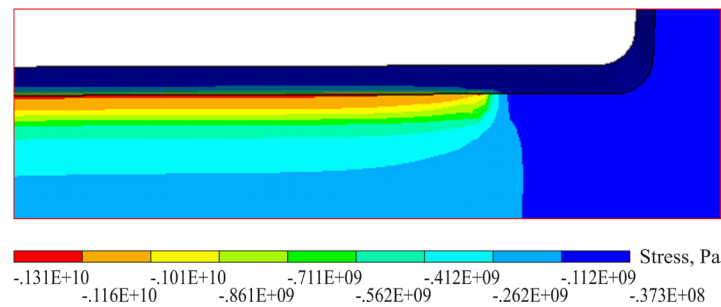


Fig. 20. The intensity of contact stresses for the optimal roller profile (enlarged)

The main result of this study is shown in Fig. 21. It shows a change in the shape of a crown if the refined multi-contact load distribution model in the circumferential direction is applied.

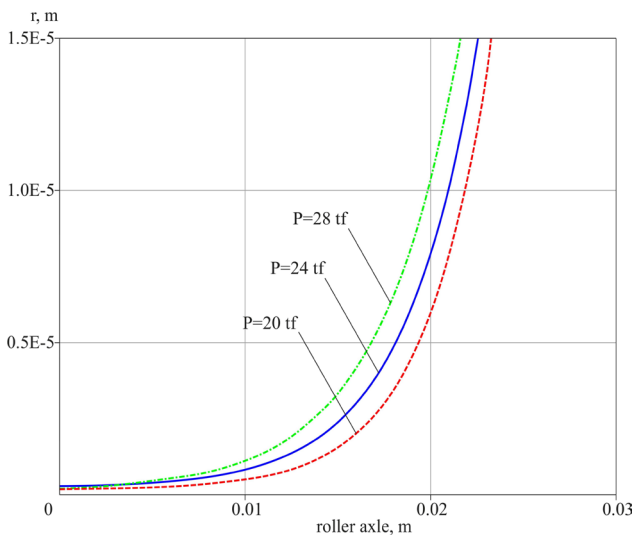


Fig. 21. Change in the shape of a roller "crown" in the case of using the refined multi-contact model

As already indicated, the refined model is characterized by a more even distribution of loads in the circumferential direction, which leads to a lower value of the maximum load on a roller than that in the simplified model. Therefore, the application of the refined model is tantamount to investigating the impact of loading a roller on the optimal shape of the roller profile. As can be seen from the comparison of the optimization results, the greater the load, the more convex the optimal crown of the roller. In this case, the maximum stresses are reduced by 15 % compared to a standard roller.

5. 2. Optimization of the roller end rounding in order to reduce wear in the axial contact with the working flange of the ring

The axial contact between the end of the roller and the working flange of the ring is characterized by mixed friction (sliding and rolling) in contrast to the contact between the roller and the raceway of the rings, where there is almost pure friction of rolling (with small adjustments to the difference in the length of the path during the contact deformation of the roller). Therefore, the end wear of the roller, all other things being equal, is much more intense and dangerous. The wear of roller ends receives the most claims in operation. The same applies to the energy efficiency of the bearing. Mechan-

ical losses from sliding friction are much higher than those from rolling friction. Another thing is that in the cylindrical bearing unit the end contact is “activated” only at turns, slopes, and at train wiggle, while in the tapered “cassette”, as a result of the triangle of forces, the end of a tapered roller is constantly in loaded contact with the flange of the inner ring. Mechanical losses, almost completely turning into heat, cause higher temperatures of the tapered bearing unit – this is a well-known fact for experts.

First of all, it is necessary to define the mathematical criterion for optimizing a convex shape of the end. The easiest way to do this is to perform it similarly to optimizing the profile (crown) of the roller and, in a given case, to accept, as an optimization criterion, the minimization of maximum contact stresses. However, if such a criterion is used, the concomitant result of reducing maximum stresses would necessarily imply expanding a “contact spot”. It is obvious that, especially in the presence of sliding friction, such a result, characteristic of providing temporary strength, will not be optimal, either in terms of improving energy efficiency or in terms of increasing the resource of the bearing unit.

Therefore, in this study, the maximum intensity of friction forces was adopted as an objective function. Imagine a “marked point” at the working flange of the ring. During the relative rotations of the ring around the wheel axle, the axle of the roller around the inner ring, and the roller around its own axis, the “marked point” draws some friction traffic at the end surface of the roller. The calculation of this trajectory for one of the “marked points” is shown in Fig. 22, *b*.

Interestingly, exactly such a pattern can be seen on most rollers as a typical pattern of roller wear (exploiters call it “herringbone”), which confirms the correctness of the model (Fig. 23, *a, b*).

Next, the intensity of friction work along the received trajectory was integrated, taking into consideration the intersection of the contact spot, and then the intensity of friction forces for all points at the working flange was summarized, integrating it for the flange height

$$G = \int A^{fp} dh, \tag{5}$$

where

$$A^{fp} = \int f \sigma_{cont} dL. \tag{6}$$

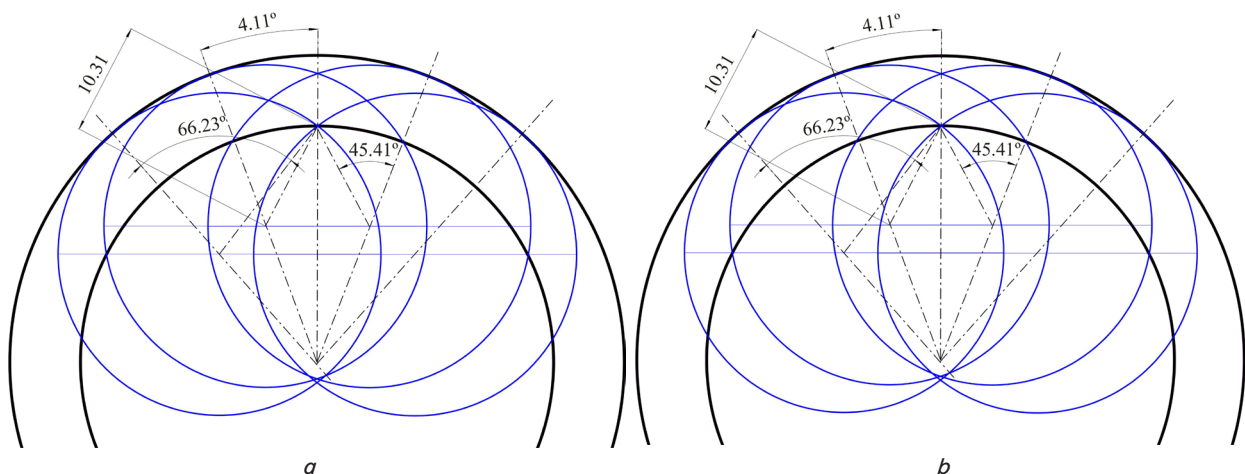


Fig. 22. Friction traffic at the end surface of the roller: *a* – calculation of reference points; *b* – trajectory synthesis

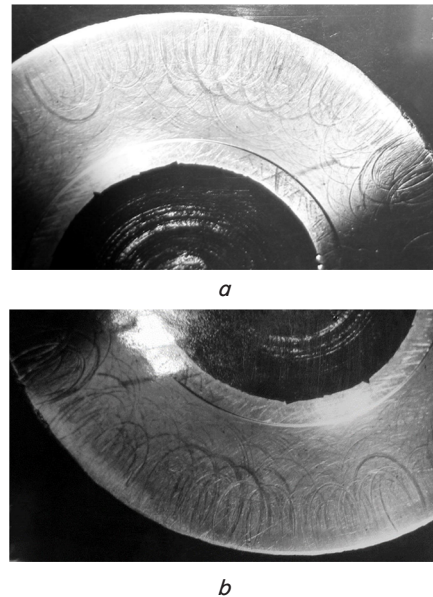


Fig. 23. Typical wear pattern of a cylindrical roller end (“herringbone”): *a* – sample No. 1; *b* – sample No. 2

Minimizing such a criterion directly corresponds to improving the energy efficiency of the node (reducing mechanical losses) and reducing wear, as it is close to the linear hypothesis of accumulating damage under irregular loading. It should be emphasized that the integration was performed for both contacts: with the working flange of the inner and outer rings. A special macros (Fig. 24) was written to calculate the integrated functionality (5) in the FEM shell of the suite. The very contact problem of analysis was solved, as geometrically non-linear, by an iterative method, and there was a much worse convergence than when calculating the contact between a roller and the raceway. The following computational technique was used to improve convergence. In the first stage, the contacting bodies are forcibly closer to a small amount without the application of an axial load (kinematic conditions). After the formation, as a result of the convergence, of the primary small contact spot, in the second stage, a full-time axial load was applied, and the problem is solved to complete convergence. The shape was optimized by the modified Nelder Mead method directly through the variation of the nodal points of the spline of the generatrix of the rotation surface.

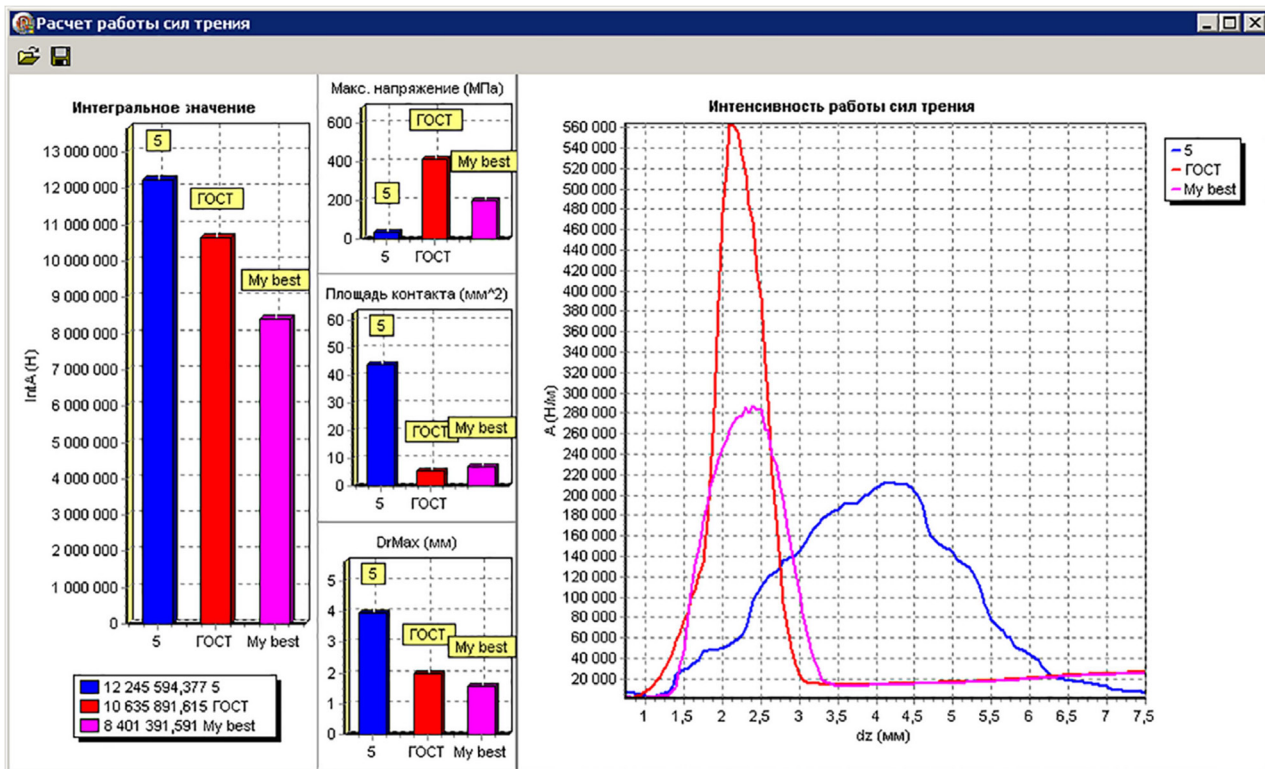


Fig. 24. The main screen of the macros (an example of the general view)

A FE model of the multi-contact problem for the end of the roller together with the flanges of the inner and outer rings is shown in Fig. 25. To reduce the dimensionality of an already costly computational task, some of the calculations were performed separately for a contact with the outer and inner ring, using a symmetry fragment.

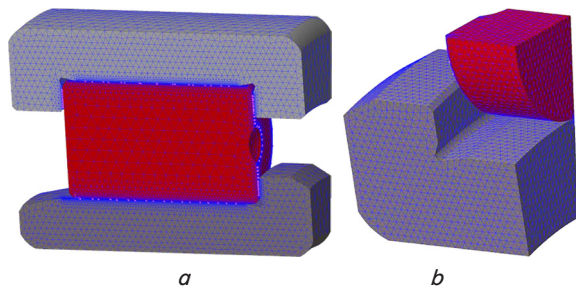


Fig. 25. A finite-element model for the multi-contact problem: *a* – model for the end of the roller together with the flanges of the inner and outer rings; *b* – fragment of symmetry

The first thing that was logical to check in the refined mathematical model, it is a long-used and experimental feature of the design of cylindrical bearings in the form of the so-called “flange camber”; a deviation of the surface of the working flange from the perpendicularity of the ring axis, which ensures the durability of the bearing.

A standard cylindrical crown roller with a flat end was taken; the surface of the working flange of the ring was varied from flat, perpendicular to the axis, to conical, with a variation of the camber of the flange from zero to 40 μm at the extreme point of the flange (0, 10, 20, 30, 40 μm), which is equivalent to the variation of angle θ (Fig. 26, *a*).

Fig. 27 shows the charts of the distribution of the intensity of friction forces for the height of the ring, as well as the diagrams illustrating the integrated value of friction forces – criterion (5), maximum stresses in MPa, the area of a contact spot in mm². Although the maximum value of wear intensity is achieved at a camber of 10 μm, the integrated criterion (5) is minimal precisely for the flange camber of 20 μm, which, while established experimentally, has been used for many years in the design and production of axlebox bearings. Next, the effect of angle α of the synchronous inclination of the flat end of the roller and the working flange of the ring was considered, retaining their above-described optimal mutual location. It was established that the optimal angle $\alpha_{opt}=2^\circ$.

In addition to the above-mentioned issues of optimizing the shape of the end contact, including the shape of the end of the roller and the return surface of the working flange, based on criterion (5), in order to improve the energy efficiency of the node (minimizing the energy of mechanical losses) and to increase the resource (minimizing wear), and the serially produced contact between the flat end of the roller and the camber of the flange of the ring (Fig. 26, *a*), the following cases were also considered:

- (B) a flat end of the roller and a convex working flange of the ring (Fig. 26, *b*);
- (C) a convex end of the roller and a conical camber of the flange (Fig. 26, *c*);
- (D) a convex end of the roller and a concave flange (Fig. 26, *d*).

The case (B) was previously considered in article [22] without taking into consideration the refined load of a multi-contact model. The rest of the procedure for introducing variable parameters, as well as the method of optimization, were kept intact.

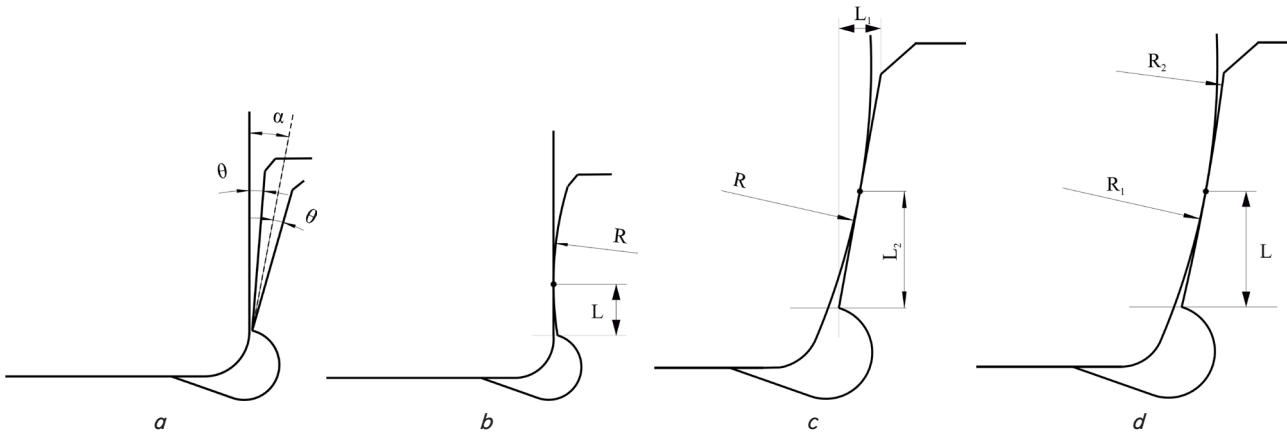


Fig. 26. Variants of contact between the roller end and the ring working flange: *a* – flat end of the roller and a flat flange of the ring; *b* – flat face of the roller and a convex working flange of the ring; *c* – convex end of the roller and the conical camber of the flange; *d* – convex face of the roller and a concave flange

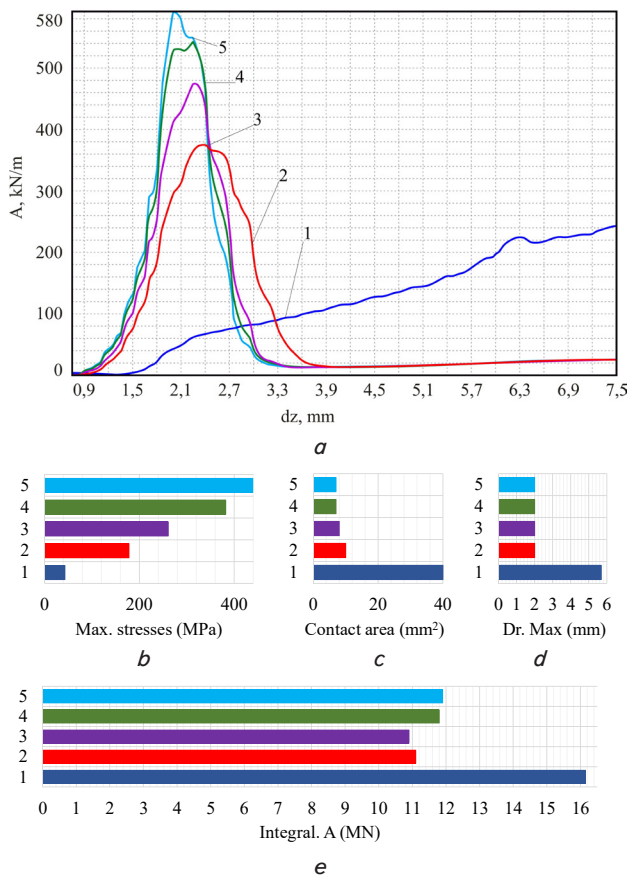


Fig. 27. Effect of the flange camber on main indicators (for the whole figure: 1 – flange camber of 0 μm , 2 – 10 μm , 3 – 20 μm , 4 – 30 μm , 5 – 40 μm): *a* – distribution charts of the intensity of friction forces for the height of the ring; *b* – maximum stresses; *c* – area of a contact spot; *d*–*e* – integrated value of the work of friction forces

The radius of the roller curvature in the contact area and the height of the point (center) of contact above the edge of the flange before the groove were selected as variable parameters for the case (C). For the case (D) – the radius of a convex end of the roller, the radius of a concave flange of the ring, and the height of the point (center) of contact above the edge of the flange.

Fig. 28 combined optimization results for all cases, including a wear pattern for the end contact of the original design of the axlebox cylindrical bearing.

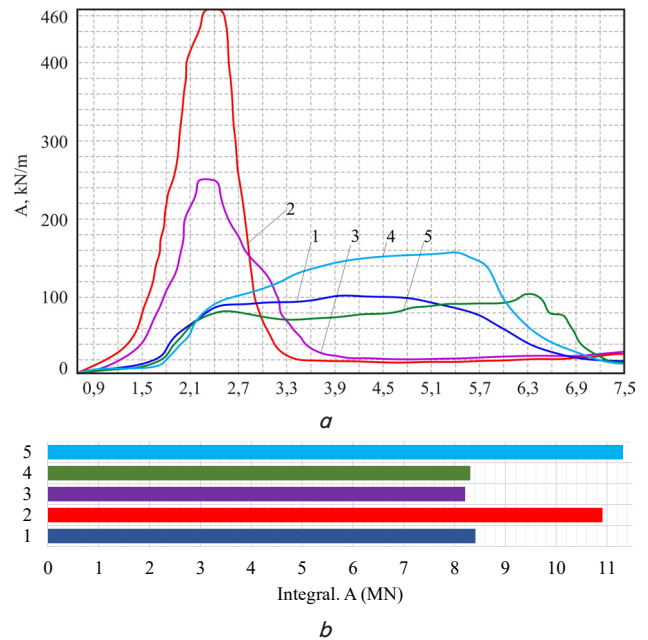


Fig. 28. Combined optimization results: *a* – charts of the intensity distribution of friction forces for the height of the ring; *b* – integrated value of the work of friction forces

6. Discussion of results of the FE simulation of a multi-contact problem

Based on the results of the FE simulation of a multi-contact problem, both the quantitative and qualitative differences have been determined in the circumferential distribution of efforts over rollers from that used in simplified models. Small gaps reveal a transition of the maximum effort from the vertical position of the roller to the position under the platform where axlebox is exposed to efforts (Fig. 9, 10). There is also the occurrence of contact load on the lower rollers as a result of the inconsistent deformation of the outer ring and the axlebox case.

Given that a contact problem is non-linear in nature, namely, geometrically non-linear, establishing the true value of the maximum load on a roller is important both for the general understanding of the loading in axlebox assembly and for finding the optimal shape of the roller profile. The greater the load, the more convex the “crown arrow”. In a given case, not any of the roller’s contacts (with the internal or external ring) was taken as critical, but rather the accumulation of damage from loading a roller in both contacts. However, as it follows from Fig. 18, the differences caused by this clarification are insignificant, which is a consequence of previously established minor differences in the optimal profile while minimizing maximum stresses from a contact with the internal or external ring.

As regards the optimization of an end contact, one can see from the comparison shown in Fig. 28 that the best results are achieved for cases (C) and (D), and, despite a different wear intensity pattern along the radius of a contact, the values of integrated criterion (5) are very close (Fig. 28, *b*). The value of the integrated criterion is somewhat better for case D, which can be termed “anthropological” (resembling a human joint). However, this difference does not justify the technological difficulties of making a concave flange. Thus, one can consider the best solution to be the combination “B – a conical flange of the ring with an optimal camber and a convex end of the roller with an optimal rounding and the optimal coordinate of a contact point”. The values of the optimal curvature radius and the coordinates of the starting contact point are within $R_{opt} \approx 3.7 \dots 4.2$ m and $L_{2opt} \approx 1.2 \dots 1.3$ mm, depending on the load on the axle and gaps in the bearing.

7. Conclusions

1. An original non-linear FE model of the multi-contact problem has been built, taking into consideration, in addition to the simultaneous contact between all rollers and the internal and outer ring, the following: the contact deformations “rail–wheel”, the deformation of a wheel axle, the deformation of axlebox and the bearing rings in contact interaction with all rollers. Unlike most works, which consider only an isolated contact “roller–ring” or “a row of

rollers–rings”, this model makes it possible not only to refine the distribution of loads in the circumferential direction and, accordingly, the maximum load on a roller for different designs of the “loader”, but also the multi-loading over the rows, the impact of gap difference and distortion. It has been established that the effect of the shape of axlebox on the distribution in the circumferential direction is significant. The same model could be used to analyze the wear of a wheel flange, as well as the reciprocal effect of the trolley elements on the SSS bearing unit and vice versa.

2. Most often, the accepted criterion for optimizing the “crown” (profile) of a roller is the condition for a minimum of maximum contact stresses. This criterion produced, on simplified models, the long-known “logarithmic” and “enhanced logarithmic” profiles. This study reports a new mathematical profile optimization model with an objective function that reflects the accumulation of damage from the “irregular” loading of the roller’s surface points in contacts with both the outer and inner ring. This criterion removes the problem of selecting which contact should be considered critical because it takes into consideration the accumulation of damage from all loads.

3. The axial contact of the end of the roller with the working flange of the ring is the weakest point of the cylindrical bearing, because, unlike the tapered bearing, which accepts a significant part of the axle load on the contact between a raceway and the roller, in the cylindrical node the axial loading is entirely accepted by the end of the roller. To optimize the surface of the roller’s end and the “response surface” of the working flange of the ring, a new criterion has been employed – a minimum of the intensity of friction forces, reflecting the intensity of wear. It is the prevention of wear that is the main requirement for closed bearings. The result of numerical optimization has established that “anthropological shapes” are the optimal ones – a convex end of the roller and a concave flange of the ring. For the technological simplification of the design, instead of the concave flange of the ring, a variant with a conical surface of the flange with the optimal “camber” value has been accepted. These shapes were patented before the industrial development of mass production of “Duplex” [20–23], and the specific values of the radii of curvature and the camber of the flange constitute a trade secret.

References

- Harris, T. A., Kotzalas, M. N. (2006). Essential Concepts of Bearing Technology. CRC Press, 392. doi: <https://doi.org/10.1201/9781420006599>
- Brändlein, J., Eschmann, P., Hasbargen, L., Weigand, K. (1999). Ball and Roller Bearings: Theory, Design and Application. Wiley, 642.
- Harnoy, A. (2002). Bearing Design in Machinery. Engineering Tribology and Lubrication. CRC Press, 664. doi: <https://doi.org/10.1201/9780203909072>
- Mason, M. A., Cartin, C. P., Shahidi, P., Fetty, M. W., Wilson, B. M. (2014). Hertzian Contact Stress Modeling in Railway Bearings for Assorted Load Conditions and Geometries. 2014 Joint Rail Conference. doi: <https://doi.org/10.1115/jrc2014-3846>
- Yang, K., Zhang, G., Wang, Y. W., Cai, S. (2019). Finite element analysis on contact stress of high-speed railway bearings. IOP Conference Series: Materials Science and Engineering, 504, 012073. doi: <https://doi.org/10.1088/1757-899x/504/1/012073>
- Gopalakrishnan, T., Murugesan, R. (2015). Contact analysis of roller bearing using finite element method. Vels Journal of Mechanical Engineering, 2 (2), 30–33. Available at: https://www.researchgate.net/publication/305768098_CONTACT_ANALYSIS_OF_ROLLER_BEARING_USING_FINITE_ELEMENT_METHOD
- Pandiyarajan, R., Starvin, M. S., Ganesh, K. C. (2012). Contact Stress Distribution of Large Diameter Ball Bearing Using Hertzian Elliptical Contact Theory. Procedia Engineering, 38, 264–269. Available at: <https://cyberleninka.org/article/n/531103>
- Shah, D. B., Patel, K. M., Trivedi, R. D. (2016). Analyzing Hertzian contact stress developed in a double row spherical roller bearing and its effect on fatigue life. Industrial Lubrication and Tribology, 68 (3), 361–368. doi: <https://doi.org/10.1108/ilt-06-2015-0082>

9. Nabhan, A., Ghazaly, N. (2015). Contact Stress Distribution of Deep Groove Ball Bearing Using ABAQUS. *Journal of the Egyptian Society of Tribology*, 12 (1), 49–61. Available at: https://www.academia.edu/25070023/Contact_Stress_Distribution_of_Deep_Groove_Ball_Bearing_Using_ABAQUS
10. Pușcașu, A. M., Lupescu, O., Bădănac, A. (2017). Analysis of cylindrical roller bearings design in order to optimize the classical process using FEM. *MATEC Web of Conferences*, 112, 06017. doi: <https://doi.org/10.1051/mateconf/201711206017>
11. Li, S., Motooka, M. (2017). A finite element method used for contact analysis of rolling bearings. *The 8th International Conference on Computational Methods (ICCM2017)*. Available at: <https://www.sci-en-tech.com/ICCM2017/PDFs/2199-9211-1-PB.pdf>
12. Demirhan, N., Kanber, B. (2008). Stress and Displacement Distributions on Cylindrical Roller Bearing Rings Using FEM#. *Mechanics Based Design of Structures and Machines*, 36 (1), 86–102. doi: <https://doi.org/10.1080/15397730701842537>
13. Hao, X., Gu, X., Zhou, X., Liao, X., Han, Q. (2018). Distribution characteristics of stress and displacement of rings of cylindrical roller bearing. *Proceedings of the Institution of Mechanical Engineers, Part C: Journal of Mechanical Engineering Science*, 233 (12), 4348–4358. doi: <https://doi.org/10.1177/0954406218820551>
14. Lin, F., Zhao, Y. X. (2008). Finite Element Analysis on the Fatigue Stresses of a Railway Vehicle Roller Bearing. *Advanced Materials Research*, 44-46, 935–941. doi: <https://doi.org/10.4028/www.scientific.net/amr.44-46.935>
15. Chen, G., Wang, H. (2016). Contact stress and radial stiffness of a cylindrical roller bearing with corrected roller generator. *Transactions of the Canadian Society for Mechanical Engineering*, 40 (5), 725–738. doi: <https://doi.org/10.1139/tcsme-2016-0059>
16. Tong, V.-C., Hong, S.-W. (2017). Modeling and analysis of double-row cylindrical roller bearings. *Journal of Mechanical Science and Technology*, 31 (7), 3379–3388. doi: <https://doi.org/10.1007/s12206-017-0627-x>
17. Simson, E. A., Anatskiy, Yu. P., Ovcharenko, V. V., Trohman, M. V., Zenkevich, Yu. A. (2009). Optimizatsiya obrazuyushchey poverhnosti rolika podshipnika kacheniya. *Vestnik Nats. tehn. un-ta "KhPI"*, 30, 8–11. Available at: http://library.kpi.kharkov.ua/files/Vestniki/2009_30.pdf
18. Simson, E. A., Anatskiy, Yu. P., Ovcharenko, V. V., Trohman, M. V., Zenkevich, Yu. A. (2009). Optimizatsiya bortov kolets i tortsevoy poverhnosti rolika podshipnika kacheniya. *Vestnik Nats. tehn. un-ta "KhPI"*, 42, 8–11. Available at: http://library.kpi.kharkov.ua/files/Vestniki/2009_42.pdf
19. Wang, Z. W., Meng, L. Q., Hao, W. S., Zhang, E. (2010). Finite Element Method Analysis and Optimal Design of Roller Convexity of Tapered Roller Bearing. *Advanced Materials Research*, 139-141, 1079–1083. doi: <https://doi.org/10.4028/www.scientific.net/amr.139-141.1079>
20. Girshfeld, A. M., Anatskiy, Yu. P., Simson, E. A., Ovcharenko, V. V. (2009). Pat. No. 44588. Method for designing optimal geometric parameters of contacting end surfaces of roller bearing. No. u200903804; declared: 17.04.2009; published: 12.10.2009, Bul. No. 19.
21. Ovcharenko, V. V., Simson, E. A., Girshfeld, A. M., Anatskiy, Yu. P. (2009). Pat. No. 44969. Method for designing optimal geometric parameters of generatrix of working surface of roller of roller bearing. No. u200903761; declared: 17.04.2009; published: 26.10.2009, Bul. No. 20.
22. Girshfeld, A. M., Rukavishnikov, V. F., Semykin, S. I., Shcherbina, A. V. (2009). Pat. No. 2425767 RF. Buksoviy podshipnikoviy uzel. declared: 14.12.2009; published: 10.08.2011.
23. Girshfeld, A. M., Simson, E. A., Ovcharenko, V. V. (2010). Pat. No. 98790 RF. Rolikoviy podshipnik.